Earthquake Geotechnical Engineering for Protection and Development of Environment and Constructions – Silvestri & Moraci (Eds)
© 2019 Associazione Geotecnica Italiana, Rome, Italy, ISBN 978-0-367-14328-2

Effect of water content and dry density to seismic behavior of homogeneous dam models in centrifuge shaking model tests

Y. Kohgo, T.T. Win, T. Sato & K. Eguchi
Tokyo University of Agriculture and Technology, Tokyo, Japan

H. Tagashira
National Agriculture and Food Research Organization, Ibaraki, Japan

ABSTRACT: We conducted a series of homogeneous dam model centrifuge shaking tests. Silica sand No. 6 and DL clay were used and the models with a different water content and density were tested. In SD series (silica sand models with a different density), the higher density might inhibit the failure slides. The higher density the larger amplitude ratios of accelerations. As the applied acceleration increased, more power water pressures (PWPs) accumulated at the centers of embankments. In SW series (silica sand models with a different water content), the models after the tests deformed roundly and the crests settled largely. The large PWP changes occurred during shaking. The differences of both behaviors were small. In DW series (DL clay models with a different water content), the model shapes after the tests depended on the water content but the maximum PWPs induced by seismic motions were almost the same. Large PWP changes also occurred during shaking but the values were smaller than those in SW series.

1 INTRODUCTION

In order to address the seismic behavior of fill dams due to strong motions categorized Level II earthquakes, which are defined as motions with huge magnitudes but low frequency to occur in service, we should know the fundamental seismic properties of the embankments. The embankments are generally constructed by compacting geo-materials (soils and rocks). These materials at first exist under unsaturated conditions. With impounding of reservoir water, some parts in the upstream reach to nearly saturated condition and others especially in the downstream remain in unsaturated one. Then the seismic behavior of the embankments may be very complex and unexpected damages may be induced during earthquake due to different seismic properties between saturated and unsaturated soils. However, there is few experimental model data about these research topics, because we have had little information about unsaturated soil mechanics, especially dynamic behavior of unsaturated soils.

During the last three decades, some important advances in the static mechanical behavior of unsaturated soils have been done (e.g. JGS 2004, Fredlund & Rahardjo 2012). We can exactly measure negative pore water pressures (exactly matric suction), clarify the suction effects to the mechanical behavior and develop elastoplastic models of unsaturated soils (Kohgo et al. 1993a & b). We may reasonably explain and understand the behavior of unsaturated soils by using the elastoplastic model (Kohgo et al. 2010a & b, Hori et al. 2011).

The dynamic properties of unsaturated soils remain out of the developments. Few researches for dike, road and railway embankments were conducted (e. g. Higo et al. 2015). In this paper, we conducted a series of homogeneous dam shaking model tests under centrifuge conditions: total 7 cases, in order to obtain the fundamental seismic properties of embankment dams.

2 CENTRIFUGE SHAKING MODEL TESTS FOR EMBANKMENTS OF DAMS

In this study, the centrifuge apparatus, which belongs to National Agriculture and Food Research Organization in Japan, was used. The effective rotation radius is 4.8m, the maximum centrifuge acceleration is 100G, and the maximum amplitude is $\pm 4.22mm$. The inner dimensions of the steel soil tank mounted on the shaking table are 60cm in height, 140cm in width and 40cm in depth. In the tests, two materials: silica sand (silica sand No. 6) and artificial silt (DL clay) were used. The physical properties and the grading curves of the materials are shown in Table 1 and Figure 1, respectively. The soil models were constructed under prescribed conditions in the soil tank with a transparent glass surface on its front side. The models are mimic homogeneous earth dams. The model conditions are shown in Table 2. The dimensions of the models were 20cm in height, 5cm in crest width and slopes of both sides were the same: 1:2.5 for 2 cases and 1:1.5 for other 5 cases. The details of the model dimensions and sensor locations are illustrated in Figure 2. Accelerations, displacements and pore water pressures (PWPs) were measured during the experimental tests. The PWPs were monitored with seven PWP transducers (Capacity = 150kPa). Each transducer was connected to each ceramic cup with a thin tube (Outer diameter = about 3mm) filled with deaired water. The size of the ceramic cup was 12.5mm in diameter and 25mm in length, while the air entry value was about 100kPa. The ceramic cups were saturated with deaired water under a vacuum. The ceramic cups were installed into the model for every experimental test. The positions of the ceramic cups (P1 – P7) installed are also shown in Figure 2. The level of each ceramic cup installed was the same as that of each connected transducer mounted within the soil tank.

In SD series, the silica sand models compacted with three different density: relative density D_r = 0, 50 and 80%, and the same initial water content w = 5% named as Cases SD1 – SD3 were used. In SW series, the models with the two different water content: w = 3 and 5%, and the same relative density D_r = 50% named as Cases SW1 and SW2 were used. In DW series,

Table 1. Material properties

Material	Silica Sand No.6	DL clay
Soil perticl density ρ_s(g/cm^3)	2.66	2.65
Max of dry density ρ_{dmax} (g/cm^3)	1.68	1.52
Minimum of dry density ρ_{dmin} (g/cm^3)	1.40	–
Optimum water content w_{opt} (%)	18.4	20.9
Sand content (%)	98.9	0.10
Silt content (%)	1.1	90.4
Clay content (%)	–	9.50
Max of particle size (mm)	0.85	0.10
60% particle size (mm)	0.35	0.02
30% particle size (mm)	0.27	0.01
10% particle size (mm)	0.17	0.00

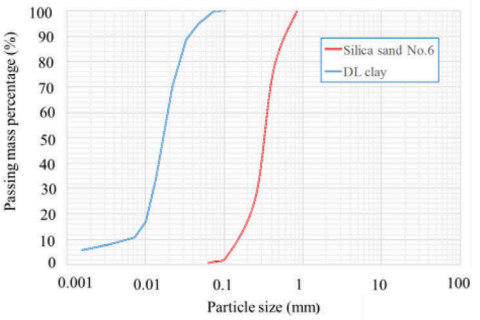

Figure 1. Grading curves of materials.

Table 2. Centrifuge model test cases

Series	Cases	Dry density ρ_d(g/cm^3)	Relative density D_r (%)	Compaction D (%)	Water content w (%)	Degree of Saturation S_r (%)	Model* type	Input** wave
SD	SD1	1.40	0	–	5	14.8	b	II
	SD2	1.53	50	–	5	18.0	b	II
	SD3	1.63	80	–	5	20.7	b	II
SW	SW1	1.53	50	–	3	10.8	a	I
	SW2	1.53	50	–	5	18.0	a	I
DW	DW1	1.30	–	84	17	43.7	c	II
	DW2	1.30	–	84	29	77.1	c	II

* See Figure 2,
** **See Table 3

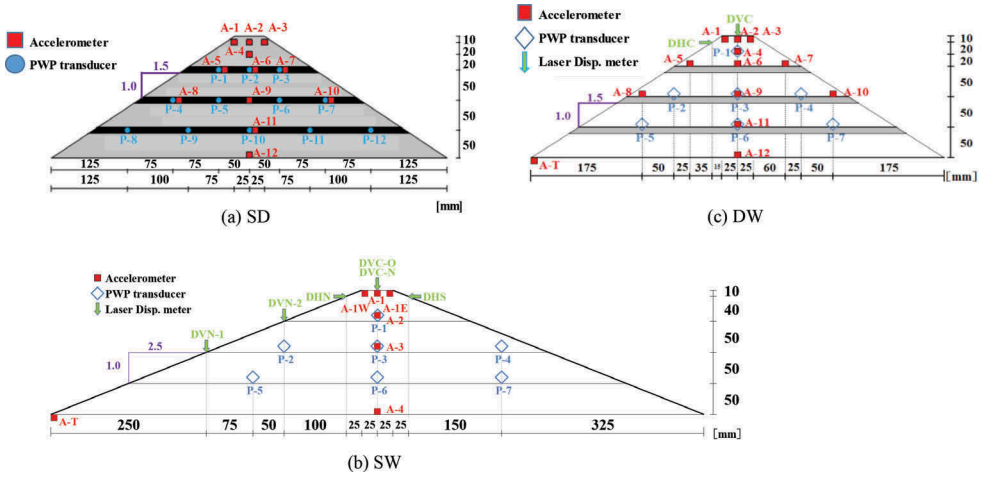

Figure 2. Cross sections of models.

Table 3. Summaries of input waves. (Data were expressed in Prototype scale.)

Input wave types	Curve type	Frequency (Hz)	Duration (s)	First input force α_1(gal)	Interval of input force $\Delta\alpha$(gal)	Final input force α_f(gal)	Example of wave
I	Sine Wave	4	3.25	100	25~100	550 or 650	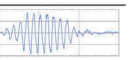
II	Sine Wave	10	6.00	300	200	500 or 700 900	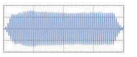

two DL clay models with the same dry density ρ_d = 1.30g/cm^3 and the different water content: w = 17% and 29% named as Cases DW1 and DW2 were adopted. After the model was set in the centrifuge apparatus, the 30G centrifuge acceleration was applied to the model. After the steady state of the model was established, the shaking tests started. The shaking direction was only up and down streams. The waves applied were summarized in Table 3.

3 RESULTS OF CENTRIFUGE SHAKING MODEL TESTS

In all the cases, scales were converted to prototype.

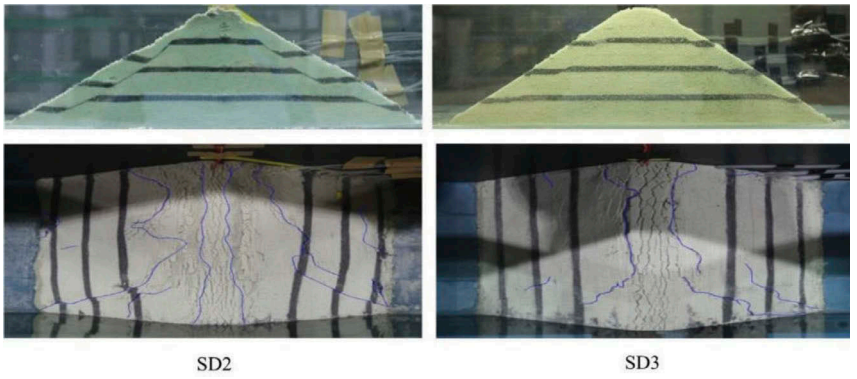

Figure 3. Failure situations of SD2 and SD3 cases.

3.1 *SD series*

In SD series, we investigated effect of dry density to dynamic properties of the dam models. Figure 3 shows failure situations of SD2 and SD3 cases after the tests. In SD1, no failure appeared and the crest of the model largely settled. It was found from Figure 3 that the larger and clearer failure lines in SD2 than those in SD3, appeared in both sides. Namely in SD3, where the relative density was larger than that in SD2, the higher density might inhibit the failure slides. The maximum depth and moving distance of the failure lines in SD2 reached 1.5m and about 1.0m, respectively, while in SD3 they were about 0.2m and 0.3m, respectively. In the crests, many cracks appeared in both cases.

Figure 4 shows the amplitude ratio of maximum acceleration. The acceleration values were measured along the center of the cross section and the datum was the value measured on the base. The values increased with elevation levels at 100gal applied and the higher density the larger ratios. At 700gal, the ratios became rather smaller and in SD1 the ratios expressed that the values were less than 1. Namely the responses of accelerations became smaller than the input accelerations.

Figure 5 shows the distributions of excess PWPs just after each shaking. As the applied acceleration increased, more PWPs accumulated at the centers of embankments in all the cases. The accumulations were larger with a decrease in density. After large accelerations were applied, excess PWPs at the crests decreased in both cases. The behavior may be related to many cracks appeared at the crests. After all the shaking, the excess PWP values remained within only ranges from + 4 to - 5.5kPa.

Figure 6 shows distributions of the magnitude of cumulative displacement vectors after each shaking. In SD1, large displacements accumulated at the both sides of the slopes, whereas rather small displacements appeared at only right-hand slope in SD3. The maximum magnitudes of the vectors after the final shaking (700 gal) in SD1 were around 0.30m. The

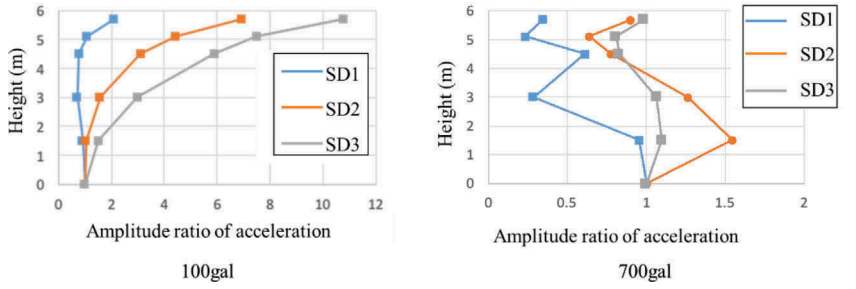

Figure 4. Amplitude ratio of maximum acceleration in SD series.

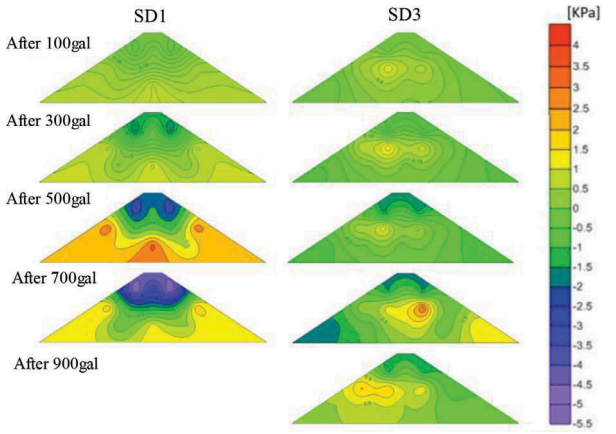

Figure 5. Distributions of PWP increments (excess PWPs) just after each shaking in SD series.

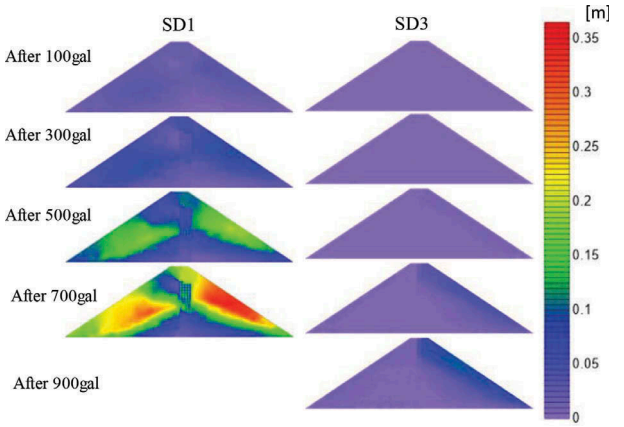

Figure 6. Distributions of the magnitude of cumulative displacement vectors.

large displacements developed at the places where the positive excess PWPs were measured. Thus, the development of displacements may be related with that of excess PWPs.

3.2 *SW series*

In SW series, we investigated effect of water content to dynamic properties of the dam models. Figure 7 shows failure situations of SW1 and SW2 cases after the tests. The models after the tests deformed roundly and the crests settled largely in both cases. The damages in SW2 were larger than those in SW1 and more cracks, which crossed each other, appeared at the crest in SW2. No clear failure lines were observed in both cases.

Figure 8 shows the amplitude ratio of maximum acceleration. The plot conditions in this figure are the same as those in Figure 4. The values at 100gal only expressed large ratios. As the same as those in SD series, at 450gal, the ratios became rather smaller and the ratios reached around 1. Thus, the responses of accelerations became smaller than the input accelerations but both behaviors were almost similar and the differences of water content between 3% and 5% were small. In this series, we selected the water content to obtain uniform distributions of water content within the models. However, we need more tests with wider range of water content.

Figures 9 and 10 show PWPs changes during 500gal shaking. Figures 9 and 10 show the results in SW1 and SW2, respectively. In both cases, the maximum PWP changes reached about

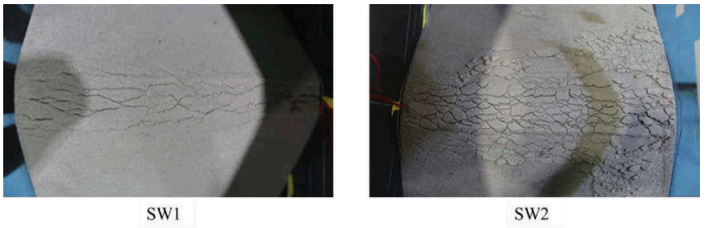

Figure 7. Failure situations in SW series.

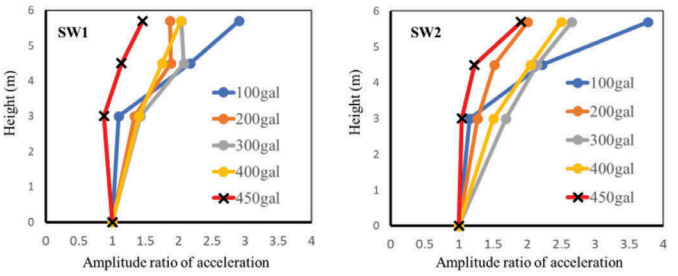

Figure 8. Amplitude ratio of maximum acceleration in SW series.

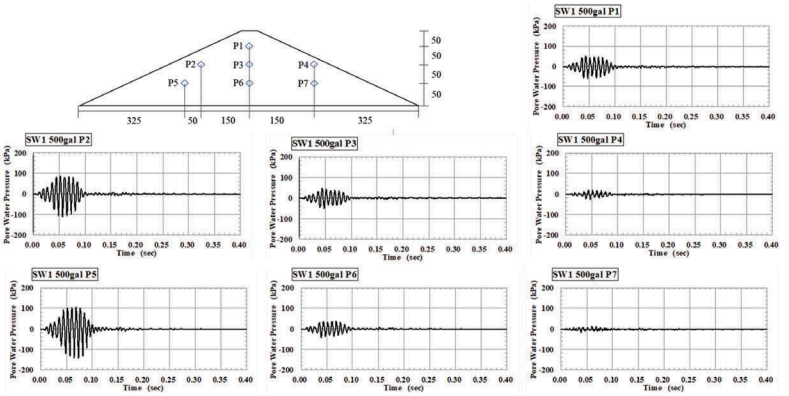

Figure 9. PWP changes during 500gal shaking in SW1 case. (Times ×30 for prototype)

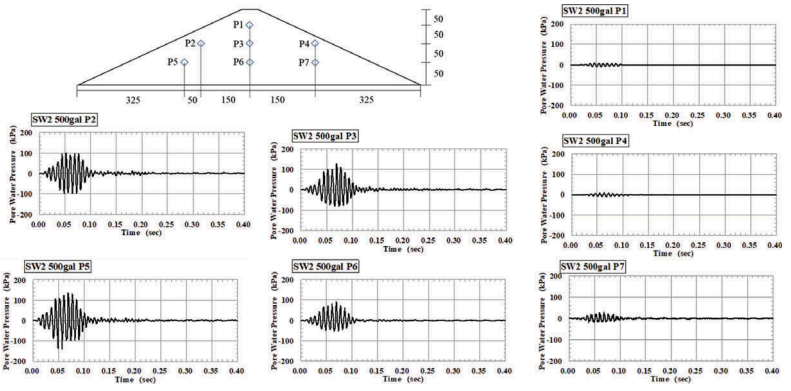

Figure 10. PWP changes during 500gal shaking in SW2 case. (Times ×30 for prototype)

$\pm 100kPa$. The changes of PWPs during shaking were larger in the left side and on the center line of the embankments. Thus, large amount of PWP changes occurred during shaking. The causes why large amount of PWP changes during shaking and the difference between right and left of the embankments occurred are now investigating.

Figure 11 shows the distributions of PWPs just after each shaking. The values before the tests monitored negative and the values in SW1were smaller than those in SW2. During the shaking, the distributions changed similarly in both cases. Namely after the values increased at the centers of the models and near bases, the values near the base largely rose and changed negative to positive. The values at the crests remained negative. After the tests, PWPs distributions in both cases were almost similar.

3.3 *DW series*

In DW series, we also investigated effect of water content to dynamic properties of the dam models. Figure 12 shows failure situations after the tests. Though surface abruptions were only seen, no clear deformations and failure were measured after several times 900gal acceleration applied in DW1. Meanwhile about 15cm settlement was measured at 300gal applied in DW2. At 500gal applied the large failure occurred and the settlement at the crest reached to 45cm. A large and vertical crack at the center of the dam axis appeared. Some cracks at lower parts of the model, which might come from the failures there, were induced.

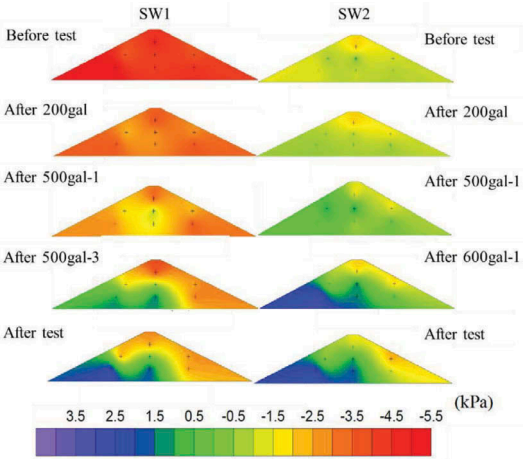

Figure 11. Distributions of PWPs just after each shaking in SW series.

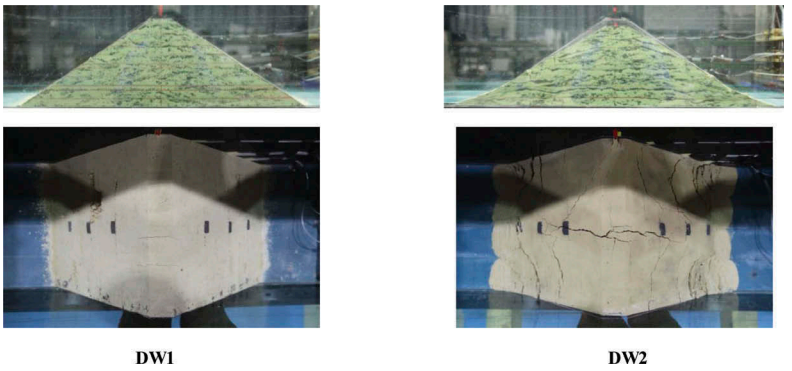

Figure 12. Failure situations in DW series.

Figure 13 shows the amplitude ratio of maximum acceleration. The plot conditions in this figure are the same as those in Figure 4. The value at the crest in DW1 had about 4 until 300gal applied. The values decreased with an increase in acceleration applied and about 1 at 900gal applied. Meanwhile the values were reduced to less than 1 at only 300gal applied in DW2. When 300gal acceleration was applied, any damages might occur within the model.

Figures 14 and 15 show PWPs changes during 500gal shaking. Figures 14 and 15 show the results in DW1 and DW2, respectively. In DW1, the initial PWPs were -30 kPa, while the

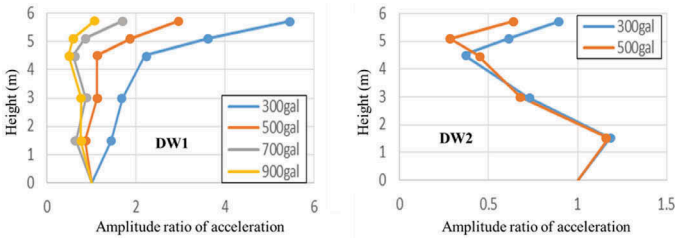

Figure 13. Amplitude ratio of maximum acceleration of DW series.

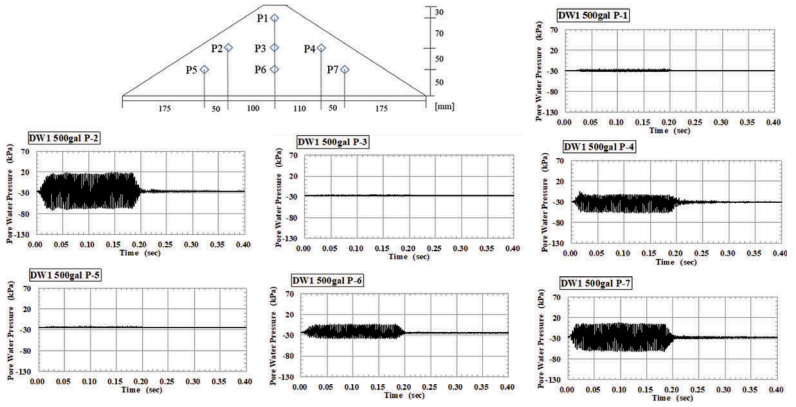

Figure 14. PWP changes during 500gal shaking in DW1 case. (Times ×30 for prototype)

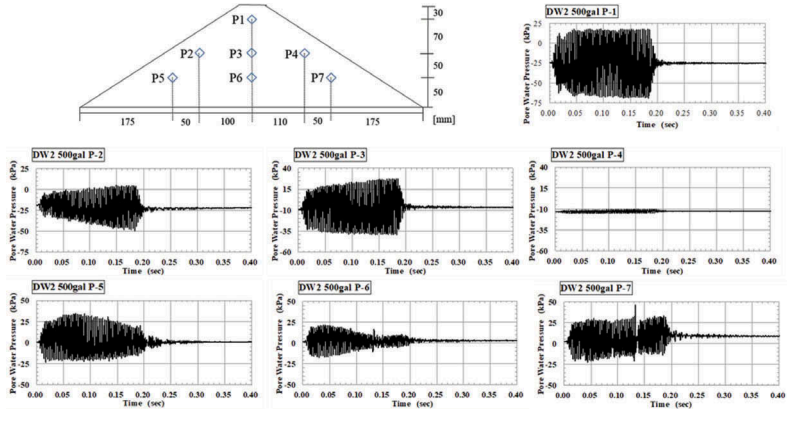

Figure 15. PWP changes during 500gal shaking in DW2 case. (Times ×30 for prototype)

values were almost zero at lower parts: P5, P6 and P7, about -10 kPa at the middle parts: P2, P3 and P4, and around -25kPa at upper part: P1 in DW2. Then, the conditions of water content at upper parts in DW2 were almost the same as those in DW1. The maximum PWP changes in DW1 and DW2 were almost the same about $\pm 40kPa$. Thus, large amount of PWP changes also occurred during shaking but the values were smaller than those in SW series.

4 CONCLUSIONS

We obtain the following conclusions from the series of these tests.

In SD series, the higher density might inhibit the failure slides. The amplitude ratios of maximum acceleration with elevation levels also depended on the densities. The higher density the larger ratios. The ratios decreased with an increase in acceleration. As the applied acceleration increased, more PWPs accumulated at the centers of embankments in all cases. The accumulations were larger with a decrease in densities. After large accelerations were applied, excess PWPs at the crests decreased.

In SW series, the models after the tests deformed roundly and the crests settled largely. No clear failure lines appeared in this series. The large amount of PWP changes occurred during shaking. The differences of behaviors were small in this series. We need more tests with wider range of water content.

In DW series, the model with w =17% did not fail at 900 gal applied but the one with w = 29% failed at 500 gal. The model shapes after the tests depended on the water content but the maximum PWPs induced by seismic motions were almost the same about $\pm 40kPa$. Thus, large amount of PWP changes also occurred during shaking but the values were smaller than those in SW series.

ACKNOWLEDGMENT

The research herein was supported by the Japan Society for the Promotion of Science (JSPS) (the grant No. 18H02296).

REFERENCES

Fredlund, D.J. & Rahardjo, H. 2012. *Unsaturated soil mechanics in engineering practice*. New York: Wiley.

Higo, Y., Lee, C.W., Doi, T., Kinugawa, T., Kimura, M., Kimoto, S. & Oka, F. 2015. Study of dynamic stability of unsaturated embankments with different water contents by centrifugal tests. *Soils & Foundations* 55(1): 112-126.

Hori, T., Mohri, Y., Kohgo, Y. & Matsushima, K. 2011. Model test and consolidation analysis for failure of a loose sandy embankment dam. *Soils & Foundations* 51(1): 53-66.

Japan Geotechnical Society (JGS) 2004. *Evaluations and behavior of unsaturated grounds*. Tokyo: Maruzen (in Japanese).

Kohgo, Y., Nakano, M. & Miyazaki, T. 1993a. Theoretical aspects of constitutive modeling for unsaturated soils. *Soils & Foundations* 33(4): 49-63.

Kohgo, Y., Nakano, M. & Miyazaki, T. 1993b. Verification of the generalized elastoplastic model for unsaturated soils. *Soils & Foundations* 33(4): 64-73.

Kohgo, Y., Takahashi, A. & Suzuki, T. 2010a. Evaluation method of dam behavior during construction and reservoir filling and the application to a real dam. *Frontiers of Architecture and Civil Engineering in China* 4(1): 92-101.

Kohgo, Y., Takahashi, A. & Suzuki, T. 2010b. Centrifuge model tests of a rockfill dam and simulation using consolidation analysis method. *Soils & Foundations* 50(2): 227-244.